Cyclic performance of viscoelastic dielectric elastomers with solid hydrogel electrodes

Yuanyuan Bai,[1] Yanhui Jiang,[2] Baohong Chen,[2] Choon Chiang Foo,[3] Yongcun Zhou,[1] Feng Xiang,[1] Jinxiong Zhou,[2] Hong Wang,[1,a)] and Zhigang Suo[4,a)]
[1]*Electronic Materials Research Laboratory, International Center for Dielectric Research, School of Electronics and Information Engineering, Xi'an Jiaotong University, Xi'an 710049, China*
[2]*State Key Laboratory for Strength and Vibration of Mechanical Structures, International Center for Applied Mechanics, School of Aerospace, Xi'an Jiaotong University, Xi'an 710049, China*
[3]*Institute of High Performance Computing, 1 Fusionopolis Way, #16-16 Connexis, Singapore, Singapore 138632*
[4]*School of Engineering and Applied Sciences, Kavli Institute of Bionano Science and Technology, Harvard University, Cambridge, Massachusetts 02138, USA*

(Received 30 October 2013; accepted 19 January 2014; published online 10 February 2014)

Hydrogels containing electrolyte can work as ionic conductors to actuate dielectric elastomer (DE) artificial muscles. Based on a popular design of a circular actuator, we study theoretically and experimentally the cyclic performance of acrylic DE actuators with solid hydrogel electrodes. The viscoelasticity of solid electrodes constrains the maximum strain that is attainable for one cycle of triangular voltage, and it also diminishes the accumulated increment of the maximum strain after many cycles of loadings. © *2014 AIP Publishing LLC*. [http://dx.doi.org/10.1063/1.4865200]

Dielectric elastomer (DE) has emerged as one of the competitive candidates for the realization of soft robotics,[1–7] adaptive optics,[8–11] actuators and sensors,[1–3,7,12–17] and generators,[18–20] due to its attractive features such as low cost, ease of manufacturing or fabrication by 3D printing, silent operation, and capability of large deformation.[1–3,6,12] Among various commercial dielectric elastomers, the VHB series acrylic elastomers by 3M Company are extensively used for prototyping or real-purpose device fabrication. This type of elastomer, however, has long been identified to be viscoelastic. Viscoelasticity of DE would affect the performance of DE devices and should be taken into account during the design stage. This aspect is crucial for applications involving dynamic input voltages, such as loudspeakers or resonators. Cyclic behavior is also closely related to the lifetime of DE. Although numerous theoretical or experimental studies on the dynamic or viscoelastic behavior of DE have been reported,[20–27] correlation between theory and experiments is still lacking. Conventional DE devices mainly use compliant electrodes made of carbon grease to drive the elastomer. Other types of electrodes have also been developed, which are all electronic conductors.[25,28–31] Recently, hydrogels containing electrolyte are used as ionic electrodes to actuate a DE loudspeaker capable of operation at frequencies beyond 10 kHz and voltages above 10 kV.[32] Motivated by this new discovery, this paper presents both experiments and analysis of cyclic viscoelastic behavior of DE actuators with solid hydrogel electrodes.

We adopt the circular configuration to investigate the performance of commercial VHB 4910 film (thickness of 1 mm) from 3M Company. Figures 1(a) and 1(b) show the schematics of the top and side views of the experimental setup. A pair of solid hydrogel electrodes was glued on the center of the prestretched circular actuator and connected to external circuits. The hydrogel electrode was synthesized following a previously reported procedure[32] by dissolving Acrylamide (AAm) monomer and lithium chloride (LiCl) powder into deionized water, and crosslinking AAm by N,N'-methylenebisacrylamide (MBAA). Lithium chloride (LiCl) was used as the electrolyte instead of sodium chloride (NaCl) because the latter dissolves out easily from the hydrogel which is disadvantageous for use. The obtained polyacrylamide (PAAm) hydrogel containing LiCl is transparent, stretchable, and conductive. The Young's modulus of the hydrogel is 1.8 kPa, the maximum rupture stretch is over 20, and the measured limiting molar conductivity is about 70 $S \cdot cm^2/mol$. Cycles of triangular waveform voltages as shown in Figure 1(c) were applied to the actuator. Figures 1(d)–1(f) present the snapshots of DE with hydrogel electrodes corresponding to the initial voltage-off state, voltage-on states for cycle 1, and cycle 30, respectively. As a comparison, Figures 1(g)–1(i) present the snapshots of DE with carbon grease electrodes corresponding to the initial voltage-off state, voltage-on states for cycle 1, and cycle 30, respectively. The enlargement of the electrode area reflects the areal strain of the actuator, which could be calculated by $\varepsilon_{areal} = S/S_0 - 1$, where S and S_0 are the electrode area of the actuator at real-time state and the initial voltage-off state, respectively.

As the applied voltage given in Figure 1(c) ramps up from zero to its peak and then goes down to zero again to complete one cycle, the areal strain of the actuator increases first to reach its maximum value and then decreases gradually. As the voltage ramps down and becomes zero again, the elastomer retains a residual strain due to viscoelasticity. The measured areal strain is recorded up to 30 cycles and three typical cycles are shown in Figure 2(a). Under a fixed voltage ramping rate of 250 V/s, the time history of the areal strain is shown in Figure 2(b), where open blue circles denote experimental data and the red solid line shows the

a)Electronic addresses: hwang@mail.xjtu.edu.cn and suo@seas.harvard.edu.

simulation result. Figures 2(a) and 2(b) indicate that both residual and maximum strains increase as the number of cycle increases, and eventually they reach their steady-state values.

The simulation result in Figure 2(b) is obtained by adopting the previously developed rheological models of DE,[33] and incorporating the elasticity of the solid electrodes,[25] and since the hydrogel electrodes are viscoelastic, the viscosity of the hydrogel electrodes is also incorporated in the present study to make the model more accurate. The DE is approximated by a rheological model with two parallel units: one unit consists of a spring with shear modulus μ^{α}, and another unit consists of a spring with shear modulus μ^{β} and a dashpot with viscosity η. The hydrogel electrode is also approximated by a rheological model with two parallel units: one unit consists of a spring with shear modulus μ^{γ}, and another unit consists of a spring with shear modulus μ^{δ} and a dashpot with viscosity η_g. The Gent model is used to represent all springs, with $J^{\alpha}_{\lim}$, $J^{\beta}_{\lim}$, $J^{\gamma}_{\lim}$, $J^{\delta}_{\lim}$ being the four corresponding extension limits, respectively.[34] The original thickness of DE is H_0, and it becomes $H_1 = H_0/\lambda_p^2$ after an equibiaxial prestretch, λ_p. The combined thickness of the hydrogel electrodes is H_2, with the volume fraction of DE and electrodes defined as $\phi_1 = H_1/(H_1 + H_2)$ and $\phi_2 = 1 - \phi_1$, respectively. Incorporating the effects of electrode viscoelasticity and assuming a homogeneous deformation state, the constitutive relation of the DE-hydrogel composite system is

$$\lambda_p^{-1}\sigma_p\lambda + \phi_1\varepsilon H_0^{-2}V^2\lambda^4 = \phi_1\left[\frac{\mu^{\alpha}\left(\lambda^2-\lambda^{-4}\right)}{1-\left(2\lambda^2+\lambda^{-4}-3\right)/J^{\alpha}_{\lim}}+\frac{\mu^{\beta}\left(\lambda^2\xi^{-2}-\lambda^{-4}\xi^4\right)}{1-\left(2\lambda^2\xi^{-2}+\lambda^{-4}\xi^4-3\right)/J^{\beta}_{\lim}}\right] + \phi_2\left[\frac{\mu^{\gamma}\left(\lambda^2\lambda_p^{-2}-\lambda^{-4}\lambda_p^4\right)}{1-\left(2\lambda^2\lambda_p^{-2}+\lambda^{-4}\lambda_p^4-3\right)/J^{\gamma}_{\lim}}+\frac{\mu^{\delta}\left(\lambda^2\lambda_p^{-2}\xi_g^{-2}-\lambda^{-4}\lambda_p^4\xi_g^4\right)}{1-\left(2\lambda^2\lambda_p^{-2}\xi_g^{-2}+\lambda^{-4}\lambda_p^4\xi_g^4-3\right)/J^{\delta}_{\lim}}\right], \quad (1)$$

where $\varepsilon = 4.11 \times 10^{-11}$ F/m, the permittivity of DE; λ, the overall stretch of DE (the same as the stretch of spring α); V, applied voltage; $\sigma_p = \frac{\phi_1\mu^{\alpha}\left(\lambda_p{}^2-\lambda_p{}^{-4}\right)}{1-\left(2\lambda_p{}^2+\lambda_p{}^{-4}-3\right)/J^{\alpha}_{\lim}}$, the stress needed to attain a prestretch, λ_p, and set as a constant in simulation; ξ, the stretch in the dashpot. The stretch of spring β is determined by adopting a multiplication rule as λ/ξ. The dashpots are modeled as Newtonian fluids, and the rate of deformation is related to stress via

$$\frac{d\xi}{\xi dt} = \frac{1}{\eta}\frac{\phi_1\mu^{\beta}\left(\lambda^2\xi^{-2}-\lambda^{-4}\xi^4\right)}{1-\left(2\lambda^2\xi^{-2}+\lambda^{-4}\xi^4-3\right)/J^{\beta}_{\lim}}, \quad (2)$$

$$\frac{d\xi_g}{\xi_g dt} = \frac{1}{\eta_g}\frac{\mu^{\delta}\left(\lambda^2\lambda_p^{-2}\xi_g^{-2}-\lambda^{-4}\lambda_p^4\xi_g^4\right)}{1-\left(2\lambda^2\lambda_p^{-2}\xi_g^{-2}+\lambda^{-4}\lambda_p^4\xi_g^4-3\right)/J^{\delta}_{\lim}}. \quad (3)$$

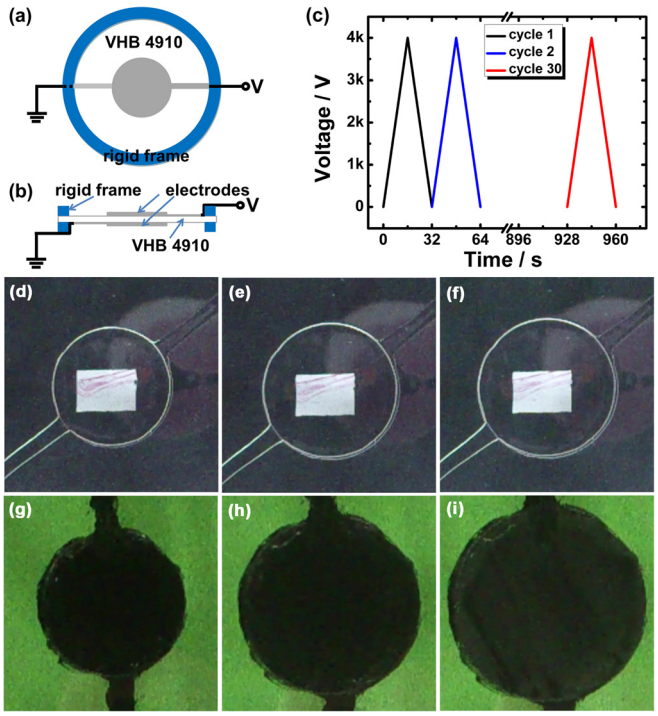

FIG. 1. Experimental setup of a circular DE actuator. (a) and (b): schematics of the top and side views of the setup; (c): applied cyclic triangular waveform voltage in experiments; (d), (e), and (f): photos of DE with hydrogel electrodes corresponding to the voltage-off state, voltage-on states for cycle 1, and cycle 30, respectively; (g), (h), and (i): photos of DE with carbon grease electrodes corresponding to the voltage-off state, voltage-on states for cycle 1, and cycle 30, respectively. The hydrogel electrodes are stretchable and transparent. The white scale is used for reference in experiments.

Equation (1) recovers the relation for a DE with compliant electrodes, e.g., carbon grease, by letting $\phi_2 = 0$ and $\phi_1 = 1$, such that the electrode thickness and the constraining effects of electrodes are negligible. The parameters used in our simulation are as following,

$\mu^{\alpha} = 17$ kPa, $\mu^{\gamma} = 0.6$ kPa, $J^{\alpha}_{\lim} = 110$, $J^{\beta}_{\lim} = 55$, $J^{\gamma}_{\lim} = 500$, $J^{\delta}_{\lim} = 500$, $\eta = \tau_V \cdot \mu^{\beta}$, $\eta_{Vg} = \tau_{Vg} \cdot \mu^{\delta}$, τ_V, and τ_{Vg} are parameters reflecting the relaxation time, τ_{vg} = 10 s, μ^{β}, μ^{δ}, τ_V, are related to the voltage ramping rate. For voltage ramping rate of 250V/s, 500V/s, and 1kV/s, μ^{β} is 38kPa, 50kPa, and 62kPa, respectively; μ^{δ} is 0.18kPa, 0.19kPa, and 0.22kPa, respectively; τ_V is 640s, 320s, and 160s, respectively.

It is intriguing to compare the cyclic performance of DE with hydrogel electrodes to that of DE with carbon grease electrodes. This comparison shows clearly the effects of elastomeric electrodes on the viscoelastic deformation of DE. Figure 3(a) plots both simulation and experimental results of DE with hydrogel and carbon grease electrodes. The ramping rate is 250 V/s and the amplitudes of applied voltage are 4 kV for 0.5 mm thick hydrogel electrodes, and 3.5 kV and

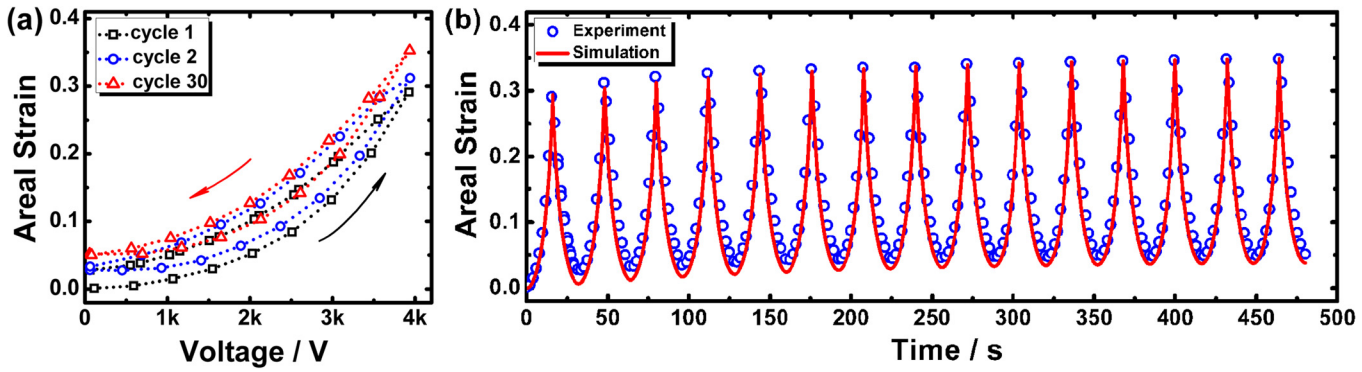

FIG. 2. Viscoelastic performance of a circular DE actuator with 0.5 mm thick hydrogel electrodes under cyclic voltages. (a): Areal strain versus voltage for three typical cycles (cycles 1, 2, and 30, respectively; ramping rate: 250 V/s); (b): Comparison of experiment and simulation of the time history of areal strain (open blue circle: experiment, red solid line: simulation; ramping rate: 250 V/s).

4 kV for carbon grease electrodes. The cyclic maximum strain evolves gradually, starting from the first maximum strain that is achieved after cycle 1, to its steady-state value indicated by the plateau. The constraining effect due to the solid hydrogel electrodes on the actuation is significant: at 4 kV, the maximum strain of each cycle for DE with hydrogel electrodes is always far less than that with carbon grease electrodes. Similarly, it is outperformed by carbon grease electrodes at 3.5 kV. Figure 3(a) also suggests that the viscoelasticity of solid electrodes diminishes the increase of the cyclic maximum strain: at 4 kV, the shift from the first maximum strain to the plateau of maximum strain for DE with hydrogel electrodes is only 0.06, which is much smaller than that of 0.26 for DE with carbon grease electrodes, and it is still smaller even if when the amplitude of applied voltage decreased to 3.5 kV for DE with carbon grease electrodes, where the first maximum strains for DE with both electrodes are almost the same. Both experimental and simulation results confirm the above effect.

To demonstrate the effect of the ramping rate on the cyclic performance of DE, systematic experiments for both hydrogel electrodes and carbon grease electrodes were carried out. Figure 3(b) shows both simulation and experimental results of the evolution of maximum strain of DE with carbon grease electrodes and hydrogel electrodes, respectively. At constant amplitude of 4 kV, we varied the ramping rates to be 250 V/s, 500 V/s, and 1000 V/s. It shows that the shifts from the first maximum strain to the plateau of maximum strain depend on the voltage ramping rate and type of electrodes. For carbon grease electrodes, the shift from the first to the steady-state maximum strain decreases with increasing voltage ramping rate, which is due to the relaxation of elastomer. Under low ramping rate, the elastomer has enough time to relax after every cycle, and the accumulated relaxation becomes larger after many cycles. Conversely, the elastomer does not have enough time to respond under fast ramping rates, such that the relaxation does not fully develop and exhibits smaller shift. However for hydrogel electrodes, the shifts are approximately the same for all three voltage ramping rates. Similar to the conclusion of Figure 3(a), this rate-independence also suggests that the viscoelasticity of solid electrodes diminishes the increase of the cyclic maximum strain. Experimental data and simulation results correlate well for the hydrogel electrodes; however, there are deviations between theoretical and experimental results for the carbon grease electrodes. The source of deviation is due to the way that prestrain is generated in the DE, which is constrained within a rigid frame (Figures 1(a) and 1(b)). Theory assumes the prestretched DE is subject to a constant biaxial stress σ_p. However, this assumption of constant σ_p does not hold under larger actuation. The stresses in the passive region surrounding the active region of the DE relax and become

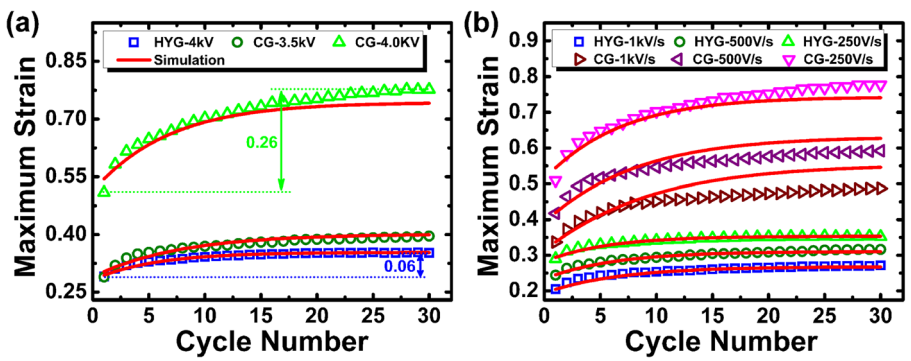

FIG. 3. Effects of elastomeric electrodes on the maximum areal strain of DE actuators. (a): Comparison of cyclic maximum strains for carbon grease electrodes and 0.5 mm thick hydrogel electrodes. The applied ramping rate is fixed to 250 V/s. The marked shift is the difference between the first and the steady-state maximum strain; (b): The effects of ramping rate on the evolution of cyclic maximum strains. The amplitude of applied voltage is fixed to be 4 kV and the ramping rates are varied to be 250 V/s, 500 V/s, and 1000 V/s, respectively. HYG denotes hydrogel electrodes, while CG denotes carbon grease electrodes. The markers are experimental results, while the red solid lines are the simulation results.

inhomogeneous. This inhomogeneous stress state is not taken into account in our current model, which requires the solution of a more complicated boundary-value problem.[35]

In summary, we study both theoretically and experimentally the cyclic performance of an acrylic elastomer. Polyacrylamide hydrogels containing LiCl salt work as ionic conductors to actuate the dielectric elastomer. The viscoelasticity of the solid electrodes and the ramping rate of applied triangular voltages are found to influence the residual and maximum strains of a circular actuator. Compared with carbon grease electrodes, the hydrogel solid electrodes constrain electro-actuation deformation and diminish the increase of cyclic maximum strain of elastomer. Good correlation between experiment and simulation is achieved. These results will help the analysis and assessment of performance of dielectric elastomer actuators subject to dynamic electric loadings.

This research was supported by Natural Science Foundation of China (Grant Nos. 61025002, 11072185, 11372239, and 11321062). Z.S. acknowledges the support of NSF MRSEC (DMR-0820484) and visiting appointment at the International Center for Applied Mechanics.

[1]R. Pelrine, R. Kornbluh, Q. B. Pei, and J. Joseph, Science **287**, 836 (2000).
[2]R. Pelrine, R. Kornbluh, J. Joseph, R. Heydt, Q. B. Pei, and S. Chiba, Mater. Sci. Eng., C **11**, 89 (2000).
[3]R. Pelrine, R. Kornbluh, and G. Kofod, Adv. Mater. **12**, 1223 (2000).
[4]H. R. Choi, K. Jung, S. Ryew, J. D. Nam, J. Jeon, J. C. Koo, and K. Tanie, IEEE/AAME Trans. Mechatron. **10**, 581(2005).
[5]I. A. Anderson, T. A. Gisby, T. G. McKay, B. M. O'Brien, and E. P. Calius, J. Appl. Phys. **112**, 041101 (2012).
[6]J. Rossiter, P. Walters, and B. Stoimenov, Proc. SPIE **7287**, 72870H (2009).
[7]P. Brochu and Q. B. Pei, Macromol. Rapid Commun. **31**, 10 (2010).
[8]F. Carpi, G. Frediani, S. Turco, and D. De Rossi, Adv. Funct. Mater. **21**, 4152 (2011).
[9]S.-i. Son, D. Pugal, T. Hwang, H. R. Choi, J. C. Koo, Y. Lee, K. Kim, and J.-D. Nam, Appl. Opt. **51**, 2987 (2012).
[10]S. Shian, R. M. Diebold, and D. R. Clarke, Opt. Express **21**, 8669 (2013).
[11]M. Heimann, H. Schroeder, S. Marx, and K.-D. Lang, Proc. SPIE **8622**, 862209 (2013).
[12]R. Shankar, T. K. Ghosh, and R. J. Spontak, Soft Matter **3**, 1116 (2007).
[13]J. Kwangmok, K. J. Kim, and C. H. Ryeol, Sens. Actuators, A **143**, 343 (2008).
[14]S. Laflamme, M. Kollosche, J. J. Connor, and G. Kofod, Struct. Control Health Monit. **19**, 70 (2012).
[15]Y. Iskandarani and H. R. Karimi, IEEE Sens. J. **12**, 2616 (2012).
[16]D. Kim, C. H. Lee, B. C. Kim, D. H. Lee, H. S. Lee, N. Canh Toan, U. K. Kim, N. Tien Dat, H. Moon, J. C. Koo, J.-d. Nam, and H. R. Choi, Proc. SPIE **8687**, 86872J (2013).
[17]T. A. Gisby, B. M. O'Brien, and I. A. Anderson, Appl. Phys. Lett. **102**, 193703 (2013).
[18]T. Mckay, B. O'Brien, E. Calius, and I. Anderson, Appl. Phys. Lett. **97**, 062911 (2010).
[19]T. G. McKay, B. M. O'Brien, E. P. Calius, and I. A. Anderson, Appl. Phys. Lett. **98**, 142903 (2011).
[20]C. C. Foo, S. J. A. Koh, C. Keplinger, R. Kaltseis, S. Bauer, and Z. G. Suo, J. Appl. Phys. **111**, 094107 (2012).
[21]P. Sommer-Larsen, G. Kofod, M. H. Shridhar, M. Benslimane, and P. Gravesen, Proc. SPIE **4695**, 158–166 (2002).
[22]J. W. Fox and N. C. Goulbourne, J. Mech. Phys. Solids **56**, 2669 (2008).
[23]A. York, J. Dunn, and S. Seelecke, Smart Mater. Struct. **19**, 094014 (2010).
[24]C. C. Foo, S. Q. Cai, S. J. A. Koh, S. Bauer, and Z. G. Suo, J. Appl. Phys. **111**, 034102 (2012).
[25]M. Bozlar, C. Punckt, S. Korkut, J. Zhu, C. C. Foo, Z. Suo, and I. A. Aksay, Appl. Phys. Lett. **101**, 091907 (2012).
[26]H. M. Wang, M. Lei, and S. Q. Cai, J. Appl. Phys.**113**, 213508 (2013).
[27]H. S. Park and T. D. Nguyen, Soft Matter **9**, 1031 (2013).
[28]F. Carpi, P. Chiarelli, A. Mazzoldi, and D. De Rossi, Sens. Actuators, A **107**, 85 (2003).
[29]S. Rosset, M. Niklaus, P. Dubois, and H. R. Shea, Adv. Funct. Mater. **19**, 470 (2009).
[30]D. C. Hyun, M. Park, C. Park, B. Kim, Y. Xia, J. H. Hur, J. M. Kim, J. J. Park, and U. Jeong, Adv. Mater. **23**, 2946 (2011).
[31]S. Michel, B. T. T. Chu, S. Grimm, F. A. Nueesch, A. Borgschulte, and D. M. Opris, J. Mater. Chem. **22**, 20736 (2012).
[32]C. Keplinger, J.-Y. Sun, C. C. Foo, P. Rothemund, G. M. Whitesides, and Z. Suo, Science **341**, 984 (2013).
[33]H. Wei, J. Mech. Phys. Solids **59**, 637 (2011).
[34]A. N. Gent, Rubber Chem. Technol. **69**, 59 (1996).
[35]S. J. A. Koh, T. Li, J. Zhou, X. Zhao, W. Hong, J. Zhu, and Z. Suo, J. Polym. Sci., Part B: Polym. Phys. **49**, 504 (2011).